

# Postprocessing treatments to improve the laser damage resistance of fused silica optical surfaces and SiO<sub>2</sub> coatings

Wenwen Liu (刘文文)<sup>1,2</sup>, Chaoyang Wei (魏朝阳)<sup>1,\*</sup>,  
Kui Yi (易葵)<sup>1</sup>, and Jianda Shao (邵建达)<sup>1</sup>

<sup>1</sup>Key Laboratory of Materials for High Power Laser, Shanghai Institute of Optics and Fine Mechanics,  
Chinese Academy of Sciences, Shanghai 201800, China

<sup>2</sup>Graduate School of Chinese Academy of Sciences, Beijing 100039, China

\*Corresponding author: siomwei@siom.ac.cn

Received November 27, 2014; accepted February 12, 2015; posted online March 24, 2015

The combination of deep wet etching and a magneto-rheological finishing (MRF) process is investigated to simultaneously improve laser damage resistance of a fused-silica surface at 355 nm. The subsequently deposited SiO<sub>2</sub> coatings are researched to clarify the impact of substrate finishing technology on the coatings. It is revealed that a deep removal proceeding from the single side or double side had a significant impact on the laser-induced damage threshold (LIDT) of the fused silica, especially for the rear surface. After the deep etching, the MRF process that followed does not actually increase the LIDT, but it does ameliorate the surface qualities without additional LIDT degradation. The combination guarantee both the integrity of the surface's finish and the laser damage resistance of the fused silica and subsequent SiO<sub>2</sub> coatings.

OCIS codes: 140.3330, 140.3440, 140.3380.

doi: 10.3788/COL201513.041407.

Improving the laser damage resistance of fused silica optical surfaces and their subsequent coatings at 3 $\omega$  has been a quest for several decades. The improved surfaces and coatings could be used in high-peak-power laser systems, such as the one at the National Ignition Facility<sup>[1]</sup>. Previous research shows that the absorption defects in the redeposition layer and the subsurface defects hidden under the redeposition layer can generate laser damages at more than two orders of magnitude lower than the intensity needed to achieve an intrinsic breakdown<sup>[2-4]</sup>. The use of etching and magneto-rheological finishing (MRF) to remove these defects separately has met with some success. In 1997, Yoshiyama *et al.* showed that the removal of up to 200 nm from the silica surface with wet etching resulted in an increase in the damage threshold. These improvements are likely due to the removal of the impurities in the polishing or redeposition layers<sup>[5]</sup>. However, further etching often resulted in a decrease rather than an increase in the damage threshold. This group hypothesized that this was possibly due to the extra etching uncovering further contaminants, more subsurface damage, and/or redepositing the contaminants<sup>[6-8]</sup>. Other researchers later showed that hydrofluoric (HF) etching could be an effective method to mitigate pre-existing damage sites. Suratwala *et al.* found that 20–30  $\mu\text{m}$  of material needs to be etched to maximize the laser damage resistance of the scratch<sup>[9]</sup>, since the subsurface defects, commonly identified as scratches and digs, are acknowledged as the leading factors in lowering the laser damage resistance of fused silica. Meanwhile, in recent years, MRF has been playing a very important role in high-precision optical fabrication, with its advantages of high determinacy, no subsurface damage, and a zero-wear process<sup>[9,10]</sup>. But the

use of MRF is restricted by its small removal function and low material removal rate.

In this Letter, we use a combination of the two treatments, deep wet etching and MRF, to improve the laser damage resistance of the surface and the surface quality simultaneously, while also saving time and costs. The front and rear surfaces of the fused silica are both investigated using various postprocessing combinations. The laser resistances of the subsequent SiO<sub>2</sub> coatings on the differently processed substrates are researched as well, since single-layer coatings typically damage the interface between the substrate and coating, indicating that the substrate finishing technology can have an impact on the laser resistance of the coatings<sup>[11-13]</sup>. In addition, the damage initiations and characteristics of the fused silica and SiO<sub>2</sub> coatings under single- and multiple-pulse irradiations are specifically investigated, to further research the effects of different postprocessing treatments.

In accordance with the processing method, the fused silica samples were divided into four series. Each series had at least six samples. The thickness of the 50 mm round fused silica sample is 5 mm. The etching was conducted in a 1% HF acid and 15% ammonium fluoride (NH<sub>4</sub>F) solution in deionized water at 23°C. Series A was only a water spray combined with ultrasonic cleaning that was rinsed off using deionized water. For series B, the samples lay flat on the bottom of the container for 15 h. The upper surfaces were etched to the depth of  $\sim 20 \mu\text{m}$ , and the lower surfaces were etched to a depth of  $\sim 3 \mu\text{m}$ . Then the upper surfaces were processed with MRF with a removal depth of about  $\sim 3 \mu\text{m}$ . To eliminate the redeposited layer that formed after the MRF process, another  $\sim 200 \text{ nm}$  were etched. For series C, the two surfaces were both etched

to the depth of  $\sim 20\ \mu\text{m}$ . Series D was first processed the same as series C. Subsequently, the MRF processes were operated on both of the surfaces to the depth of  $\sim 3\ \mu\text{m}$ . Another  $\sim 200\ \text{nm}$  depth was also etched after the MRF. In addition, after the above processes, the samples in series B–D were all cleaned the same way as the sample in series A. To determine the deep etching depth, we used an electronic balance with the resolution of  $0.0001\ \text{g}$  to weigh the mass loss  $\Delta m$  of every sample before and after etching. Then, the etch depth is represented by  $\Delta h = \Delta m / (\rho \times S)$ , where  $\rho$  is the density of the fused silica and  $S$  is the surface area. For series D, the etch depth of the two surfaces are the same and easy to calculate. For series B, after we know the etch depth of one surface, which is the same as series D, the etch depth of the other surface is easy to acquire.

The  $\text{SiO}_2$  coatings were deposited via e-beam evaporation on substrates of series A and B, each with a diameter of  $50\ \text{mm}$ . The thickness of the film was about  $350\ \text{nm}$ . All coating depositions used the same deposition technology and occurred in the same coating chamber.

The laser damage test apparatus used in this study and the error analysis were both introduced in Ref. [14]. A Nd:YAG laser was used to provide  $355\ \text{nm}$  of laser light (8 ns pulse, Gaussian temporal and spatial profile). The  $1/e^2$  spot diameters on the  $x$  and  $y$  axes of the front surface were measured via the knife-edge method and were  $322$  and  $432\ \mu\text{m}$ , while those of the rear surface were  $297$  and  $390\ \mu\text{m}$ .

The damage morphologies were observed by a Zeiss scanning electron microscope. An optical profiler was also employed in mapping the root mean square (rms) micro-roughness ( $R_q$ ).

The damage probability curves of the four series of fused silica are shown in Fig. 1. Figure 1(a) shows the damage probabilities of the front surfaces. Compared to series A, the damage probabilities of the samples in series B, C, and D decrease distinctly, and are almost at the same level. This shows that the  $\sim 20\ \mu\text{m}$  removal eliminates the most dangerous precursors, inducing low-density laser damages, to some extent, while significantly increasing the laser damage resistance. The next MRF process ensures the quality of the highly precise optical surfaces without the generation of new subsurface damage. Meanwhile, the other  $\sim 3\ \mu\text{m}$  removal during the MRF process does not improve the laser-induced damage threshold (LIDT) further. It is notable that the laser resistance of series B is

nearly the same as that of the samples in series D. This indicates that the deep removal from a single side is sufficient for the front surface of the LIDT, which is likely generally unaffected by the condition of the rear surface. Thus, considering the time and effect, the subsequent  $\text{SiO}_2$  coatings are deposited on the substrates of series A and B. The damage probabilities of the rear surface shown in Fig. 1(b) mainly exhibit the same trends as those of the front surface. Deep etching significantly improves the LIDTs of the rear surfaces. However, the samples in series B are not improved, and are even a little worse than the samples in series A. This indicates that deep removal on just one side is dangerous for rear-surface LIDT. The very different trends of the damage probabilities between the front and rear surfaces of series B demonstrate that the condition of the front surface will affect the rear surface, not vice versa. Here, we must clarify that for series B, when we test the LIDTs of the front or rear surface, the surface that has been etched up to  $20\ \mu\text{m}$  is presented on the front or rear surface, respectively. In addition, for the samples with and without postprocessing, no self-focusing effect is found in our experiment. The reason may be that the laser intensity in the samples is not high enough to cause self-focusing, since the focus of our laser is behind the samples and the self-focusing effect is proportional to the square of the laser intensity.

The specific LIDTs for the front and rear surfaces under multiple-pulse irradiations are also tested and listed in Table 1. During the course of experiment, we found that the damage sites were all initiated at the first pulse, which means that the undamaged sites will not be modified and damaged under the subsequent pulses. The results in Table 1 also verify the fact that there is no fatigue effect existing in the front and rear surface damages of the fused silica. Additionally, the LIDT of the front surface is obviously higher than that of the rear surface for each series. For front surface, the LIDTs of series B, C, and D are clearly over two times higher than that of series A. Additionally, for series C and D, the LIDTs of the rear surfaces are significantly improved. However, the results of series B reveal that removal should proceed from the double side at the same time, especially if one wants to improve the LIDT of the rear surface.

Many studies show that removal of up to  $200\ \text{nm}$  of the silica surface results in an increase in the damage

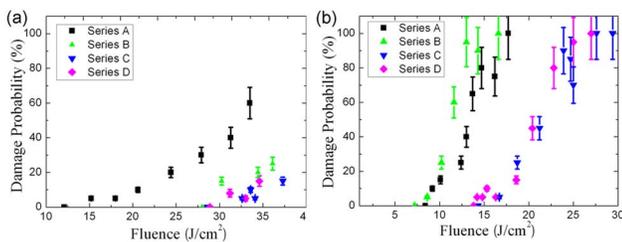


Fig. 1. Damage probabilities of (a) the front surface, and (b) the rear surface for the four series of fused silica.

**Table 1.** LIDTs of the Front and Rear Surfaces

LIDT ( $\text{J}/\text{cm}^2$ )		A	B	C	D
Front surface	1-on-1	12.1	28	28.6	28.9
	10-on-1	12.8	27.3	31.2	28
	30-on-1	12.3	28.6	28.5	26.9
Rear surface	1-on-1	8.4	7.2	14.3	14.2
	10-on-1	7.8	7.5	14.5	14
	30-on-1	9.2	8	14	14.2

threshold<sup>[11,12]</sup>. During our research, we found that this is not always true, and sometimes results in even more damage. In comparison with shallow etching, deep etching can improve the LIDT with greater confidence and to a greater degree. However, the best LIDTs of our rear surfaces still have room for improvement. Recently, Baxamusa *et al.* demonstrated that the organic damage precursors that are generated as precipitates during chemical processing steps such as cleaning, etching, and rinsing, are a limiting factor for high-quality fused silica optics. By working to exclude the reagent and process contamination and to minimize precipitation during chemical processing operations, they have produced silica optics with extraordinarily low damage densities that saturate about  $200 \text{ cm}^{-2}$  on test samples<sup>[15,16]</sup>. There is still a gap between the LIDTs of the exit surfaces reported in this work and theirs, probably because we have no unified, standard operation.

Some *S*-on-1 damage probability curves of the  $\text{SiO}_2$  coatings, with value of *S* ranging from 1 to 30, are shown in Fig. 2. Figures 2(a) and 2(b) show the results of the coatings deposited on the substrates of series A and B, respectively. It is apparent that the laser resistance of the coatings deposited on series B improved drastically. In comparison with the improvement in the fused silica, the LIDTs of the  $\text{SiO}_2$  coatings are increased by seven times, and the 100% damage probability thresholds increase by 10. This result confirms that the postprocessing treatments of the fused silica can improve the laser resistance of the front and rear surfaces and the subsequent  $\text{SiO}_2$  coatings simultaneously. In addition, the  $\text{SiO}_2$  coatings exhibit no fatigue effect, like the fused silica does.

Surface morphology and quality observations enable the precise viewing of the damage characteristics and the identification of the damage initiators. In order to clarify the reasons why the LIDTs decrease or increase under different processes, the surface conditions after different postprocessing treatments and laser irradiations are obtained.

The evolution of the surface morphologies after different etching depths for the same fused silica sample is researched, and the statistical results are shown in Fig. 3. Figures 3(a) and 3(b) illustrate the scratch and dig densities with different etching depths, respectively. Each data represents the result of at least six tested spots.

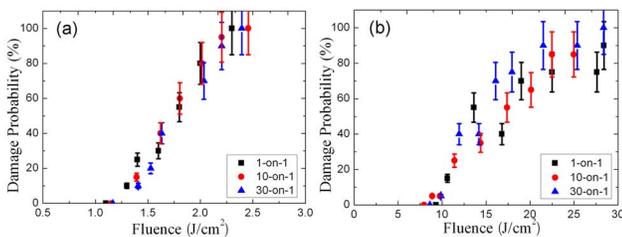


Fig. 2. Damage probabilities of  $\text{SiO}_2$  coatings deposited on the substrates of series (a) A and (b) B, which are measured on the input surface.

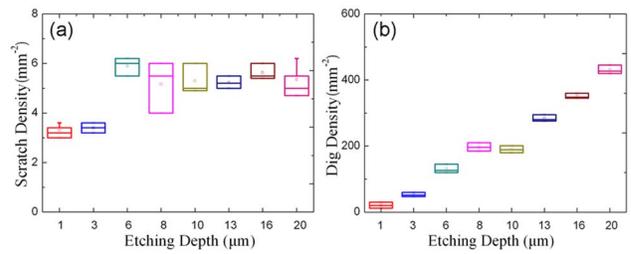


Fig. 3. (a) The scratch densities and (b) the dig densities of the same fused silica sample etched to different depths.

The densities of the exposed digs and scratches significantly increase with the etching depth. In particular, the dig density increases in a near-linear trend. The scratch density is mainly maintained at  $\sim 5 \text{ mm}^{-2}$  when the etching depth is larger than  $6 \mu\text{m}$ . However, as we mentioned above, compared with the samples in series A, the samples in series C where we removed up to  $20 \mu\text{m}$  have much higher laser resistances. This phenomenon indicates that deep etching has removed impurities in the polishing layer and subsurface defects to some extent, and that the exposed digs and scratches have no effect on the laser-induced damages. The damage morphologies also confirm this conclusion.

Figure 4(a) illustrates damage to the front surface of series A that was induced by a trailing indentation scratch consisting of banana-shaped pits<sup>[17]</sup>. The irradiated laser fluence is  $33.5 \text{ J/cm}^2$  in the 1-on-1 mode. The most dangerous damages to the front surface of series A behave like micro-pits. The samples without etching have scratches on the surface, some of which can induce damage. These scratches generally manifest as trailing indentation scratches. After the etching removes up to  $20 \mu\text{m}$  from the silica surface, the scratches all behave as continuous scratches, as shown in Fig. 4(b). From the observation of the damage morphologies, we find that these scratches and digs will no longer cause damage. The comparison of the damage probability curves of series C and D also verify this conclusion. The samples after the MRF process, in which the exposed continuous scratches and digs are all removed, show almost the same results as the samples that did not receive MRF, as shown in Fig. 1. Bercegol *et al.* deliberately created scratches on the surface of fused silica and measured the damage resistance of these scratches.

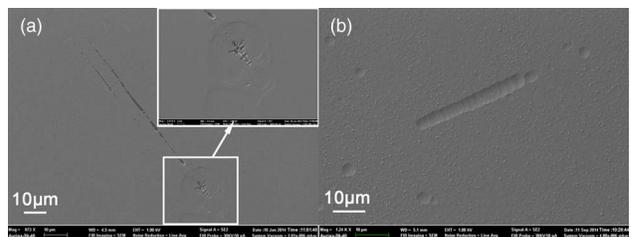


Fig. 4. Damage morphologies of the front surfaces for (a) damage sites irradiated with  $33.5 \text{ J/cm}^2$  in series A (b) undamaged sites in series C.

They demonstrated that the fracture could lead to laser damage, but that plastic deformation could not produce laser damage<sup>[17]</sup>. Thus, the continuous scratches or digs exposed by the deep wet etch process are acknowledged as plastic deformations that will not induce laser damage<sup>[18,19]</sup>. The damage morphologies and LIDTs both indicate the surface damages of series B–D are induced by invisible, nano-scaled defects. The fact that the removal of another  $\sim 3\ \mu\text{m}$  during the MRF process does not change the laser resistance illustrates that these invisible, nano-scaled defects may be traced back to the processing water and reagents used during etching and rinsing<sup>[15,16]</sup>.

The effect of the postprocessing treatments on the rear surface damage probability curves and the initiation of damage is similar to that on the front surface, except in series B. As we have mentioned above, the input surfaces of the samples in series B are only etched to  $\sim 3\ \mu\text{m}$ . This etching depth may result in a decrease rather than an increase in the damage threshold. The Yoshiyama group hypothesized that it is possibly due to the uncovering of further contaminants, of more subsurface damage, and/or redeposition of the contaminants<sup>[5]</sup>. In addition, the condition of the front surface may affect the rear surface, resulting in this freak phenomenon. However, much more work needs to be done to identify the reason.

Although the exposed scratches and digs will not induce laser damage, besides the LIDT, the surface quality must be considered after the deep etching process, especially for the fused silica, which will be used as the substrate of coatings. Figure 5 displays the rms micro-roughness ( $R_q$ ) of all of the samples in the four series. Each sample is measured at six different positions. The results of series B are measured on the surface, which is both deep etched and MRF

treated. The results show that the difference between the minimum and maximum  $R_q$  of series B is less than 0.2 nm for series A, but larger than 3 nm for series C. It is about 0.7 nm for series B and D. In addition, the maximum  $R_q$  of these four series are 0.98, 1.8, 5.87, and 1.78 nm, respectively. These very different results for the four series reveal that the removal of up to  $20\ \mu\text{m}$  from the surface has a significant effect on the surface's  $R_q$ . Despite the samples in series C having high LIDTs, the value of  $R_q$  is large. Figures 6(a)–6(c) exhibits the specific  $R_q$  mapping of series A, series C, and series D, respectively. Series B and D are considered to have the same surface conditions because they underwent the same postprocessing treatments. It is clearly that after deep etching, some big digs and scratches are exposed on the surfaces. The MRF process resolves this problem, as shown in Figs. 5 and 6, which ensures the surface quality while avoiding bringing in new subsurface defects that would decrease the LIDT<sup>[20]</sup>.

The laser damage probability curves presented in Fig. 2 verify that the laser resistance of the  $\text{SiO}_2$  coatings which have been deposited on the processed substrate is apparently improved. It is clear that the combination of deep etching and MRF can improve the laser damage resistance and ensure the highly precise optical surface of the fused silica and subsequent deposited  $\text{SiO}_2$  coatings simultaneously. The damage sites of the  $\text{SiO}_2$  coatings in the 1-on-1 case show that the initiators are from the substrate<sup>[21]</sup>. The damage morphologies of the  $\text{SiO}_2$  coatings are similar to the front surface damages of the fused silica. This is easy to understand, since the thickness of our  $\text{SiO}_2$  coatings is only 350 nm. However, because of the coupling effect of the substrate and coatings, the LIDT of the  $\text{SiO}_2$  coatings is significantly lower than that of the substrate. It should be noted that we only tested the LIDTs of the  $\text{SiO}_2$  coatings. If one wants to ensure the rear surface as well, deep etching should proceed from the double side of the substrate. Thus, the laser resistance of the optics can be improved with more confidence. In addition, for multiple-pulse irradiations, the damage sites of the  $\text{SiO}_2$  coatings are all initiated by the first pulse. The fact that there is no fatigue effect existing in the subsequent  $\text{SiO}_2$  coatings certifies that the initiators are from the substrate. As we mentioned above, these invisible nano-scaled defects, which may be from the processing water and reagents used during etching and rinsing, exhibit very different characteristics with the damage precursors in

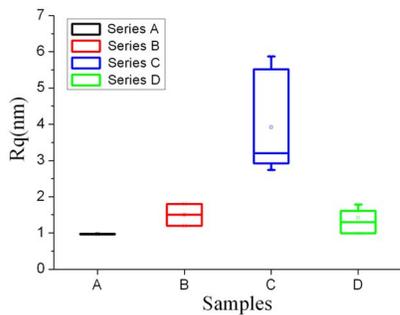


Fig. 5. The  $R_q$  of the four series.

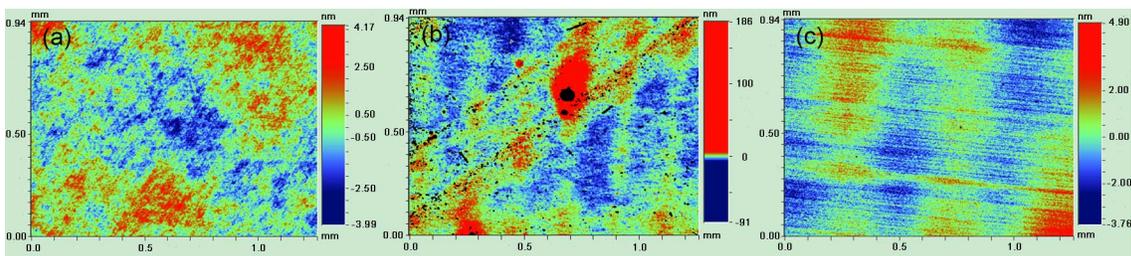


Fig. 6.  $R_q$  map of (a) series A, (b) series C, and (c) series D.

coatings that commonly exhibit the fatigue effect in nano-second regime<sup>[4]</sup>.

The laser resistances of the fused silica, including the front and rear surfaces, and the subsequent SiO<sub>2</sub> coatings are all improved after the postprocessing treatments. The investigations include various combinations of deep etching and MRF, which can proceed from either the single-side or the double side. The results show that large etched amounts can significantly improve the LIDTs. The removal can proceed from the single-side if one only wants to improve the LIDT of the front surface. But to improve the LIDT of the rear surface, deep etching should proceed from the double side. The exposed scratches and digs after deep etching will not induce further damage under the influence of laser irradiations. The MRF process ameliorates the surface qualities without additional LIDT degradation. The combination guarantees both the surface finish and the laser damage resistance of the fused silica and subsequent coatings. Additionally, the optical surface of the fused silica and SiO<sub>2</sub> coatings both exhibit no fatigue effect under multiple pulse irradiations. However, much more work is needed to identify the most appropriate etching depth to maximize the laser damage resistance under the premises of economical time and the nature of the invisible precursors.

This work was supported by the National Natural Science Foundation of China under Grant Nos. 11104293 and 61308021.

## References

1. P. E. Miller, T. I. Suratwala, J. D. Bude, T. A. Laurence, N. Shen, W. A. Steele, M. D. Feit, J. A. Menapace, and L. L. Wong, Proc. SPIE **7504**, 75040X (2009).
2. G. H. Hu, Y. A. Zhao, X. F. Liu, D. W. Li, Q. L. Xiao, K. Yi, and J. D. Shao, Opt. Lett. **38**, 2632 (2013).
3. J. Liu, W. Zhang, H. Cui, J. Sun, H. Li, K. Yi, and M. Zhu, Chin. Opt. Lett. **12**, 083101 (2014).
4. S. Papernov and A. W. Schmid, Proc. SPIE **7132**, 71321J (2008).
5. J. Yoshiyama, F. Genin, A. Salleo, I. Thomas, M. Kozlowski, L. Sheehan, I. Hutcheon, and D. Camp, Proc. SPIE **3244**, 331 (1998).
6. P. P. Hed, D. F. Edwards, and J. B. Davis, Lawrence Livermore National Laboratory Report **99548**, 1 (1989).
7. T. I. Suratwala, P. E. Miller, J. D. Bude, W. A. Steele, N. Shen, M. V. Monticelli, M. D. Feit, T. A. Laurence, M. A. Norton, C. W. Carr, and L. L. Wong, J. Am. Ceram. Soc. **94**, 416 (2011).
8. C. Battersby, L. Sheehan, and M. Kozlowski, Proc. SPIE **3578**, 446 (1999).
9. S. D. Jacobs, W. I. Kordonski, I. V. Prokhorov, D. Golini, G. R. Gorodkin, and T. D. Strafford, Magnetorheological Fluid Composition, U.S. Patent No. 5,795,212 (Sept.8, 1998).
10. D. Golini, G. Schneider, P. Flug, and M. Demarco, Opt. Photon. News **12**(10), 20 (2001).
11. G. H. Hu, S. Y. Shao, M. H. Yang, J. D. Shao, Y. A. Zhao, K. Yi, and Z. X. Fan, Proc. SPIE **7504**, 75040D (2009).
12. Z. Yu, H. He, X. Li, H. Qi, and W. Liu, Chin. Opt. Lett. **11**, 073101 (2013).
13. F. Kong, Y. Jin, S. Liu, S. Chen, H. Guan, K. He, Y. Du, and H. He, Chin. Opt. Lett. **11**, 102302 (2013).
14. W. W. Liu, C. Y. Wei, J. B. Wu, Z. K. Yu, H. Cui, K. Yi, and J. D. Shao, Opt. Express **21**, 22476 (2013).
15. S. Baxamusa, P. E. Miller, L. Wong, R. Steele, N. Shen, and J. Bude, Opt. Express **22**, 29568 (2014).
16. J. Bude, P. Miller, S. Baxamusa, N. Shen, T. Laurence, W. Steele, T. Suratwala, L. Wong, W. Carr, D. Cross, and M. Monticelli, Opt. Express **22**, 5839 (2014).
17. H. Bercegol, R. Courchinoux, M. Josse, and J. L. Rullier, Proc. SPIE **5647**, 78 (2004).
18. G. H. Hu, Y. A. Zhao, D. W. Li, Q. L. Xiao, J. D. Shao, and Z. X. Fan, Surf. Interface Anal. **42**, 1465 (2010).
19. P. E. Miller, J. D. Bude, T. I. Suratwala, N. Shen, T. A. Laurence, W. A. Steele, J. A. Menapace, M. D. Feit, and L. L. Wong, Opt. Lett. **35**, 2702 (2010).
20. D. Golini, W. I. Kordonski, P. Dumas, and S. Hogan, Proc. SPIE **3782**, 80 (1999).
21. S. Papernov and A. W. Schmid, J. Appl. Phys. **97**, 114906 (2005).